XLIII CILAMCE
21-25, November, 2022
FOZ DO IGUAÇU - PR - BRAZIL

Influence of different factors related with the train-bridge interaction system in the stability of high-speed trains subjected to strong winds

P.A. Montenegro[1], H. Carvalho[2], D. Ribeiro[3], M. Ortega[4], F. Millanes[4], J.M. Goicolea[5], W. Zhai[6], R. Calçada[1]

[1] *CONSTRUCT - LESE, Faculty of Engineering, University of Porto, Porto, Portugal*
paires@fe.up.pt; ruiabc@fe.up.pt
[2] *Department of Structural Engineering, Federal University of Minas Gerais, Belo Horizonte, Brazil*
hermes@dees.ufmg.br
[3] *CONSTRUCT - LESE, School of Engineering, Polytechnic of Porto, Porto, Portugal*
drr@isep.ipp.pt
[4] *IDEAM SA, Madrid, Spain*
miguel.ortega@ideam.es; francisco.millanes@ideam.es
[5] *School of Civil Engineering, Technical University of Madrid, Madrid, Spain*
jose.goicolea@upm.es
[6] *Train and Track Research Institute, State Key Laboratory of Traction Power, Southwest Jiaotong University, Chengdu, China*
wmzhai@home.swjtu.edu.cn

Abstract. Strong crosswinds are one of the most critical sources of excitation that may impact with the train runnability and safety. However, there are a significant number of characteristics related with the train-bridge system that are rarely addressed which may influence the train's performance when subjected to this kind of actions. The present work aims to fill this gap, by individually studying the impact of such characteristic, such as the bridge lateral stiffness and the track condition, in the runnability of high-speed (HS) trains moving over bridges subjected to crosswinds. The Arroyo de Las Piedras Viaduct, a high pier viaduct belonging in the Spanish HS network, was used as case study. The study concluded that the bridge's lateral behavior has a negligible impact in wind-induced derailments, while the track condition, considered in this work with four quality levels, proved to significantly influence the train's running safety, especially at higher speeds. This is due to the fact that the Nadal and Prud'homme indexes strongly depend on the wheel-rail lateral impacts, which become more pronounced for higher speeds and under poorer track conditions.

Keywords: train running safety; train-track-bridge interaction; high-speed railway bridges; wind loads; bridge lateral flexibility; track condition.

1 Introduction

Train derailments due to wind loads deserve singular attention, especially when the trains are crossing long viaducts with high piers, which are usually located in valleys prone to strong crosswinds that hit the train regularly. The study of train running safety in the presence of crosswinds is being studied in the past few years by several research groups, mainly in Asia and Europe. Xiang *et al.* [1] studied the protection effect caused by wind barriers in three track configurations, namely in a ground roadbed, in a high embankment and in a bridge. Zhang *et al.* [2] carried out a study to evaluate the consequences of sudden changes in the wind load due the presence of barriers. More recently, Montenegro *et al.* [3] performed a running safety study in the future Volga River HS bridge belonging to the Moscow-Kazan HS link, where the train's stability using two distinct wind models, namely the Chinese Hat model and a turbulent wind model, have been compared.
The present work aims to study several factors that may influence the train stability moving over bridges subjected to crosswinds, namely the influence of the bridge lateral flexibility and track condition. To achieve this, the Arroyo de Las Piedras viaduct, a long high-pier viaduct in the Spanish HS network, is used as main case study but is latter parameterized to simulate bridges with different lateral behaviors to understand the impact in the running safety.

Moreover, four levels of track condition, from ideal (without irregularities) to high level of irregularities, but still within the limits imposed by the codes for HS lines, are also considered.

2 Methodology for analyzing the train running safety on bridges

The current codes [4] address the train running safety with indirect indicators based on bridge response, such as vibration and displacement levels. These indicators, which are usually easily accessed through simple static or dynamic analyses, do not consider sources of excitation other than the traffic loads. Therefore, for a more precise analysis, the running safety on bridges against crosswinds should be explicitly assessed through safety indexes, which depend on the wheel-rail contact forces calculated with appropriate train-track-bridge interaction (TTBI) models. The indexes used in this work consist of the Nadal, Prud'homme and Unloading criteria, which are mathematically described in Table 1.

The dynamic analyses are performed with a TTBI numerical tool developed by Montenegro *et al.* [5]. This tool, capable of dealing with lateral dynamics, is implemented in MATLAB® and imports the structural matrices from the railway vehicle and bridge modelled in a FE package (ANSYS® in the present work). Then, the external excitations are imposed to the coupling system and the corresponding dynamic responses are obtained. The interaction between the two sub-systems is accomplished by a specially developed contact finite element that considers the behaviour of the contact interface between wheel and rail. The contact formulation is divided in three main problems, namely i) the geometrical, ii) the normal and iii) the tangential contact problems. With the contact interface fully characterized, the equations of motion of the vehicle and bridge are complemented with constraint equations that couple these two structural systems. The full mathematical formulation and validation of the TTBI model is presented in the authors' previous publications [5].

Table 1 – **S**afety criteria used in the present study to assess the train running safety.

Criterion	Criterion index	Allowances	Filter type
Nadal (relative to each wheel)	$\xi_N = \frac{Y}{Q}$	0.8	Low-pass filter with a cut-off frequency of 20 Hz using a 4th order filter after performing a sliding mean based on a window size of 2.0 m [6].
Prud'homme (relative to each wheelset)	$\xi_P = \frac{\sum_{ws} Y}{10 + \frac{2Q_0}{3}\,[\text{kN}]}$	1.0	
Unloading (relative to each side of each bogie)	$\xi_U = 1 - \frac{Q_i + Q_j}{2Q_0}$	0.9	Low-pass filter with a cut-off frequency of 2 Hz using a 4th order Butterworth filter [7].

Q_0: static vertical wheel load; Q: vertical wheel contact force; $Q_{i,j}$: vertical contact force on wheels i and j from the same side of the bogie; Y: lateral wheel contact force; $\sum_{ws} Y$: total lateral contact force by a single wheelset.

3 Wind velocity fields and loads

3.1 Stochastic generation of wind velocity fields

The wind velocity field is generated stochastically taking into account the power spectral density function S for each direction. According to Cao *et al.* [8], if the elevation is constant along the wind field and the distance between any successive wind generation points is the same, which can be perfectly adopted for the majority of the studies regarding running safety over bridges, the time-histories of the horizontal u_j and vertical v_j fluctuating components of the wind in the j^{th} generation point can be simulated by

$$u_j(t) = \sqrt{2\,\Delta\omega} \sum_{m=1}^{j} \sum_{f=1}^{N} \sqrt{S_u(\omega_{mf})}\, G_{jm}(\omega_{mf}) \cos(\omega_{mf} t + \phi_{mf}) \quad (1)$$

$$w_j(t) = \sqrt{2\,\Delta\omega} \sum_{m=1}^{j} \sum_{f=1}^{N} \sqrt{S_w(\omega_{mf})}\, G_{jm}(\omega_{mf}) \cos(\omega_{mf} t + \phi_{mf}) \quad (2)$$

where $\Delta\omega$ is the frequency increment, ω_{mf} is a double indexed frequency dependent on the frequency increment, $S_u(\omega_{mf})$ and $S_w(\omega_{mf})$ are the horizontal and vertical wind spectra defined by the Kaimal [9] and Lumley and Panofsky [10] spectra, respectively, ϕ_{mf} is a random variable phase angle uniformly distributed between 0 and 2π, N is the number of wind frequencies and $G_{jm}(\omega_{mf})$ is an element of the coefficient matrix $\mathbf{G}(\omega_{mf})$ related with the cross-spctral density matrix $\mathbf{S}(\omega_{mf})$, responsible for correlating the wind spectra of each generation point and described in detail in Cao *et al.* [8]. Details of the whole wind field generation can be consulted in the authors' previous publications [3].

3.2 Wind loads

The drag $F_{d,j}$ and lift $F_{l,j}$ wind loads per unit length applied to the bridge (see Figure 1.a) at each generation point j are given by

$$F_{d,j}(t) = \frac{1}{2}\rho\, V_j(t)^2\, C_{d,j}(\alpha)\, H_j \tag{3}$$

$$F_{l,j}(t) = \frac{1}{2}\rho\, V_j(t)^2\, C_{l,j}(\alpha)\, B_j \tag{4}$$

where $C_{d,j}(\alpha)$ and $C_{l,j}(\alpha)$ are the drag and lift aerodynamic coefficients, respectively, at the generation point j, α is the wind incidence angle, H_j and B_j are the height and width of the wind exposed area at point j, ρ is the air density and V_j is the resultant wind velocity in j dependent on the mean wind velocity $\bar{U}$ and the fluctuating components given in Eqs. (1) and (2) and that can be expressed as

$$V_j(t) = \sqrt{\left[\bar{U} + u_j(t)\right]^2 + w_j(t)^2} \tag{5}$$

The aerodynamic coefficients, these can be obtained by wind tunnel tests or, in the case of typical deck sections such as those studied in this work (rectangular box girder with slab on top), through the procedure stipulated in Section 8 from EN 1991-1-4 [11].

In relation to the moving train (see Figure 1.b), the mean $\bar{F}_f$ and fluctuating $F_f'(t)$ components of the aerodynamic forces acting on it (subscript *f* indicates drag or lift) are given by

$$\bar{F}_f = \frac{1}{2}\rho A\, C_f(\bar{\beta})\, \bar{V}_r^{\,2} \tag{6}$$

$$F_f'(t) = \rho\, A\, C_f(\bar{\beta})\, \bar{U}\left(1 + \frac{1}{2C_f(\bar{\beta})}\, C_f'(\bar{\beta})\, cot\,\bar{\beta}\right)\int_0^{\infty} h_F(\tau)\, u(t-\tau)d\tau \tag{7}$$

where A is the reference area, $C_f(\bar{\beta})$ and $C_f'(\bar{\beta})$ are the aerodynamic coefficient and its derivative, respectively, evaluated at the mean yaw angle $\bar{\beta}$, $\bar{V}_r$ is the mean relative velocity, as illustrated in Figure 1.b, and $h_F(\tau)$ is a weighting function that accounts for the effects caused by the instantaneous turbulence and by the turbulence history over a time lag τ. This function is defined in detail in [12].

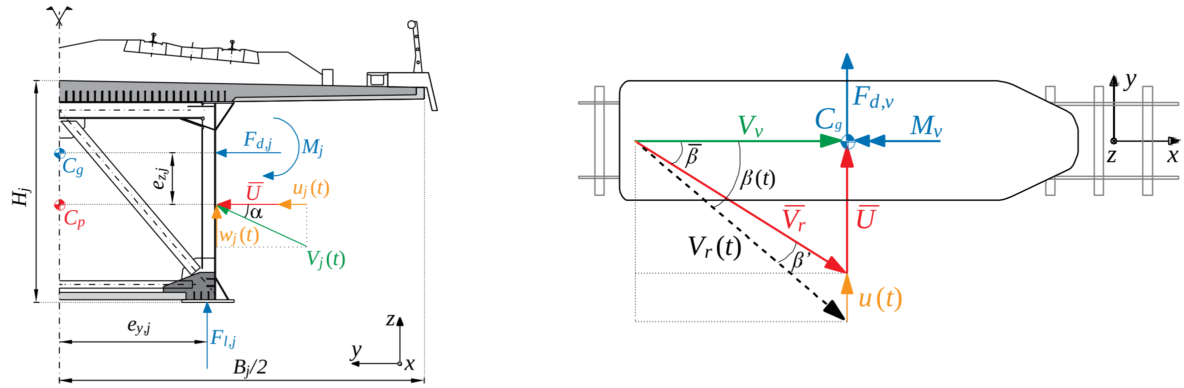

(a) (b)

Figure 1 – Wind velocity vectors and aerodynamic forces acting on the (a) bridge deck and (b) train.

4 Numerical models

4.1 Bridge model

The Arroyo de Las Piedras viaduct (see Figure 2) is a double track bridge located in Spain in the Córdoba-Málaga HS line, formed by a steel-concrete double composite action deck composed by 19 continuous spans of 50.4 + 17 × 63.5 + 44 + 35 m. Above the columns, in the negative moment zones, a bottom cast-in-place concrete slab with thickness ranging from 0.50 m to 0.25 m is added over the prefabricated slabs to increase the bending and torsional stiffness of these zones. The compression stresses in the bottom side of the cross-section that arise from the negative bending moments in these zones keep the bottom slab uncracked, which contributes to a significant improvement in the dynamic response of the viaduct, especially against the eccentric traffic loads caused by the trains running on a single track. The deck is supported by very high and slender piers, some of them over 93 m, through pot bearing devices. The cross-sections of the piers are hollow rectangles with dimensions at the top of 2.50 m and 6.70 m in the longitudinal and transversal directions, respectively. A detailed description of the viaduct's design characteristics can be found in Millanes *et al.* [13].

(a)

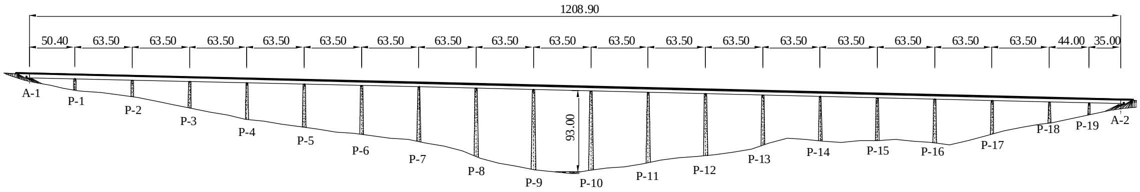

(b)

Figure 2 – The Arroyo de Las Piedras viaduct: (a) photo and (b) elevation (m).

The numerical model of the viaduct has been developed in the FE package ANSYS® using mainly beam finite elements. The cross-section properties of the deck have been homogenized in steel to allow modelling it with beam elements and keep the bending and torsional properties intact. The columns have been also modelled with beam elements with variable dimensions along their lengths according to the description presented before.

Taking into consideration the limited information available in the literature, the first main objective of the present work consists of comprehensively address the influence of the lateral flexibility of bridges in the train's running safety. To achieve this, a parameterization of the original Arroyo viaduct has been made to simulate different bridges flexibilities without losing the realistic characteristics of a HS railway bridge. By adopting the original viaduct as the base scenario to represent structures with high flexibility, three more scenarios have been defined, namely two with lower flexibilities and one with higher. Thus, for a certain scenario *i*, the relative flexibility $\Delta\delta_i$ of the corresponding model is defined in relation to the flexibility of the original structure through

$$\Delta\delta_i = \frac{\delta_i}{\delta_0} \tag{8}$$

where δ_i and δ_0 are the lateral flexibilities of the structural models from scenario *i* and original viaduct, i.e. the displacements caused by a unit lateral load at a certain location of the deck. Thus, three additional viaduct models have been developed with different pier properties to simulate the flexibility scenarios described in Table 2.

Table 2 – Studied scenarios based on the lateral flexibility of the corresponding structural model.

Scenario *i*	Description	Relative flexibility $\Delta\delta_i$ (%)
S1	Rigid viaduct	0
S2	Medium flexibility	50
S3	Original viaduct (high flexibility)	100
S4	Very high flexibility	150

4.2 Track

The ballasted track has been incorporated in the viaduct model to guarantee a smoother and more realistic load transfer between the train and the bridge. The rails and sleepers are modelled with beam elements, while the behaviour of the ballast and pads/fasteners is simulated through spring-dashpot with appropriate characteristics (the track properties adopted in this work can be consulted in [14]). The track irregularity profiles have been artificially generated according to the procedure described by Claus and Schiehlen [15]. According to these authors, the low, medium and high levels of irregularities accepted in normal operational conditions in the HS railways network in Germany are characterized by scale factors of $0.592 \times 10^{-6}\mathrm{rad/m}$, $1.089 \times 10^{-6}\mathrm{rad/m}$ and $1.586 \times 10^{-6}\mathrm{rad/m}$, respectively. Therefore, three different profiles have been generated to perform the analyses.

4.3 Train model

The present work considers the HS train that actually crosses the case study viaduct, the Siemens Velaro AVE-S103, whose axle load is 15.5 t. The numerical model of the vehicles has been developed in ANSYS®. The carbody, bogies and wheelsets are modelled as rigid bodies through rigid beam elements connected to each other through the primary and secondary suspensions defined with spring dashpot elements in the three directions.

5 Running safety analysis

The TTBI dynamic analyses have been carried out for a wide range of train speeds and wind velocities. Regarding the former, speeds between 140 km/h up to 420 km/h with 20 km/h steps were considered in the study, while the wind velocity fields were generated considering mean wind speeds ranging from 20 m/s to 30 m/s with 1 m/s steps. The main characteristics used in the stochastic generation process of the wind fields are: i) roughness length z_0 equal to 0.05 m, ii) maximum wind frequency considered f_{up} equal to 6 Hz discretized into 3000 discrete frequencies (Δf = 0.002 Hz); iii) time duration of the generated wind field equal to 10 min with 0.05 s time increments. A constant height above the ground of 55 m, equivalent to the mean height of the piers of the original viaduct, has been considered to simulate the wind velocity time-series from all the wind generation points on the deck (generation points equally spaced by 16 m).

5.1 Influence of lateral flexibility of the viaduct in the vehicle's stability

Knowing that different levels of lateral flexibility may lead to considerably different lateral responses of the superstructure, it is crucial to understand if these different behaviours also affect the train's stability. To help answering this question (Objective 1), Figure 3 depicts the critical train speeds according to each safety criteria for the four scenarios defined in Table 2 (results refer to the Siemens Velaro AVE-S103 train and to the high level of irregularities). Figure 3.d also shows the intersection of all curves to obtain the safety boundary for each scenario (continuous and dashed lines represent the critical speeds conditioned by the unloading and Prud'homme factors, respectively). It is possible to observe that the influence of the viaduct's flexibility in the train running safety is very low, since the critical train speeds obtained with all the models do not significantly vary (see the grey area in Figure 3.d). Such phenomenon may be explained by the fact that the wind acting on the bridge causes only a smooth and low frequency lateral movement to the deck, and consequently to the track, allowing the train to easily follow it due to the friction forces acting on the wheel-rail interface. This low-frequency lateral movement of the bridge is, therefore, insufficient to impose a sudden and aggressive response to the train. This is a very interesting conclusion, since it may allow significant simplifications in the structural model when the sole objective of the analysis is to study the train running safety against crosswinds.

5.2 Influence of lateral flexibility of the viaduct in the vehicle's stability

To study the influence of the track quality in the train's stability (Objective 2), the results obtained in the base scenario (original viaduct, AVE-S103 HS train and high level of irregularities) are compared with those obtained with lower irregularity levels. The safety boundaries defined by each safety criteria, and by their intersections considering the four track condition scenarios described above are plotted in Figure 4. The results allow to conclude that the critical speeds determined by the unloading factor are not significantly dependent on the track condition, since this criterion is majorly governed by low frequency overturning movements of the carbody caused by the lateral winds. However, the safety boundaries defined by the other two criteria have a strong correlation with the magnitude of the irregularities, since the contact force peaks are highly dependent on the impacts between wheel and rail that become more pronounced in poorer track conditions. Note that the unloading index is always determinant for the train safety in a perfect track scenario and for speeds up to 320 km/h when the track quality is very good (low level of irregularities), while for the medium and high levels of irregularities this index is critical only for speeds up to 220~260 km/h (the Nadal criterion, once again, is not determinant). Thus, the correct consideration of the track condition is essential to assess the maximum allowed train speeds.

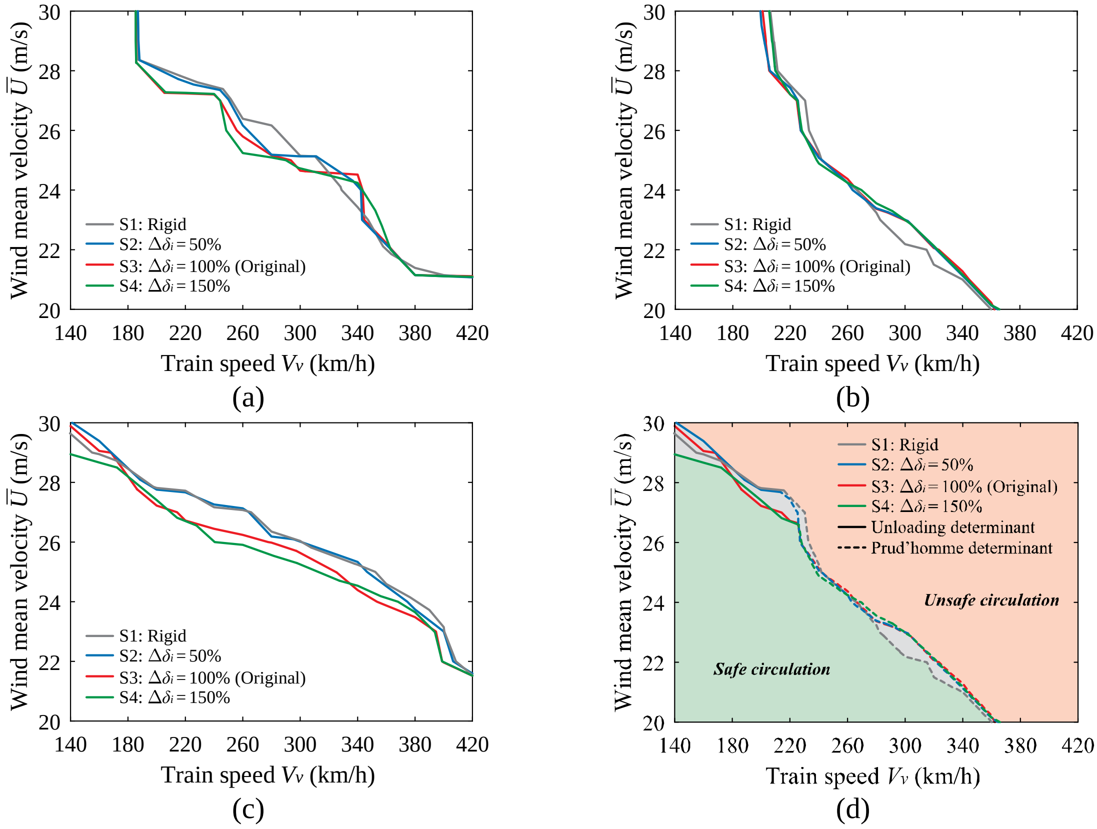

Figure 3 – Running safety boundaries for the four flexibility scenarios relative to the (a) Nadal, (b) Prud'homme and (c) unloading indexes and to the (d) intersection between them.

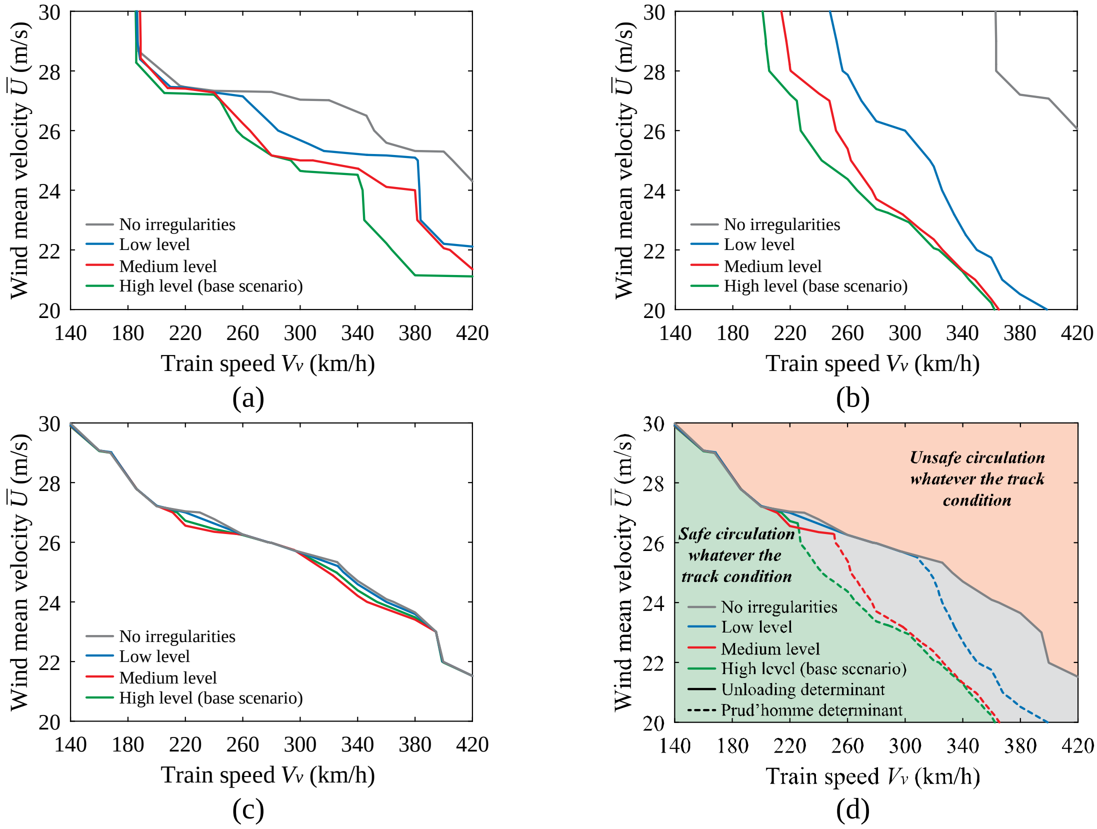

Figure 4 – Running safety boundaries for the four track condition scenarios relative to the (a) Nadal, (b) Prud'homme and (c) unloading indexes and to the (d) intersection between them.

6 Conclusions

The present paper presents a study to evaluate how different factors related to the bridge and track may influence the train running safety on bridges subjected to strong lateral winds. The running safety evaluation is carried out through three safety indexes (Nadal, Prud'homme and unloading) obtained with dynamic analyses performed with an in-house TTBI model. Two main goals were set, namely the study of the influence of the bridge lateral behaviour (Objective 1) and of the track condition (Objective 2) in the risk of derailment. From this work, the following conclusions are draw:

- Regarding Objective 1, the results shown that the risk of derailment is practically not affected by the lateral flexibility of the viaduct. Thus, simplifications on the structural model of the bridge are acceptable when the sole objective of the analysis is to study the train running safety against crosswinds.
- Regarding Objective 2, the outcomes of this work shown that the unloading criterion is not influenced by the track quality, since it is mainly governed by low frequency overturning movements of the carbody caused by the lateral wind loads. However, the remaining two indexes are strongly related to the level of the irregularities due to the higher contact forces that arise from the impacts between the wheels and rail in poorer track conditions.

Acknowledgements. This work was financially supported by: Base Funding - UIDB/04708/2020 and Programmatic Funding - UIDP/04708/2020 of the CONSTRUCT - Instituto de I&D em Estruturas e Construções funded by national funds through the FCT/MCTES (PIDDAC); Grant no. 2020.00305.CEECIND from the Stimulus of Scientific Employment, Individual Support (CEECIND) - 3rd Edition provided by ‘‘FCT – Fundação para a Ciência e Tecnologia’’. Moreover, the work was also financially supported by the projects IN2TRACK2 and IN2TRACK3 funded by the Shift2Rail Joint Undertaking under the European Union's Horizon 2020 research and innovation programme under grant agreements No. 826255 and No. 101012456, respectively.

Authorship statement. The authors hereby confirm that they are the sole liable persons responsible for the authorship of this work, and that all material that has been herein included as part of the present paper is either the property (and authorship) of the authors, or has the permission of the owners to be included here.

References

[1] Xiang H, Li Y, Chen B, Liao H, Protection Effect of Railway Wind Barrier on Running Safety of Train Under Cross Winds, Advances in Structural Engineering 2014; 17 (8): 1177-1187.
[2] Zhang T, Xia H, Guo WW, Analysis on running safety of train on the bridge considering sudden change of wind load caused by wind barriers, Frontiers of Structural and Civil Engineering 2018; 12: 558–567.
[3] Montenegro PA, Barbosa D, Carvalho H, Calçada R, Dynamic effects on a train-bridge system caused by stochastically generated turbulent wind fields, Engineering Structures 2020; 211: 110430.
[4] EN 1991-2. Eurocode 1: Actions on structures - Part 2: Traffic loads on bridges, CEN, Brussels, 2003.
[5] Montenegro PA, Neves SGM, Calçada R, Tanabe M, Sogabe M, Wheel-rail contact formulation for analyzing the lateral train-structure dynamic interaction, Computers & Structures 2015; 152: 200-214.
[6] EN 14363. Railway applications - Testing and Simulation for the acceptance of running characteristics of railway vehicles - Running Behaviour and stationary tests, CEN, Brussels, 2016.
[7] EN 14067-6. Railway applications - Aerodynamics - Part 6: Requirements and test procedures for cross wind assessment, CEN, Brussels, 2016.
[8] Cao Y, Xiang H, Zhou Y, Simulation of Stochastic Wind Velocity Field on Long-Span Bridges, Journal of Engineering Mechanics 2000; 126 (1): 1-6.
[9] Kaimal JC, Wyngaard JC, Izumi Y, Coté OR, Spectral characteristics of surface-layer turbulence, Quart. J. Royal Meteorological Society 1972; 98: 563-589.
[10] Lumley J, Panofsky H. The structure of atmospheric turbulence. Interscience Publishers, New York, 1964.
[11] EN 1991-1-4. Eurocode 1:Actions on structures-Part 1-4: General actions-Wind actions, CEN,Brussels, 2010.
[12] Baker CJ, The simulation of unsteady aerodynamic cross wind forces on trains, Journal of Wind Engineering and Industrial Aerodynamics 2010; 98 (2): 88-99.
[13] Millanes F, Pascual J, Orteja M, "Arroyo Las Piedras" Viaduct: The first Composite Steel-Concrete High Speed Railway Bridge in Spain, Structural Engineering International 2007; 17 (4): 292-297.
[14] Montenegro PA, Heleno R, Carvalho H, Calçada R, Baker CJ, A comparative study on the running safety of trains subjected to crosswinds simulated with different wind models, Journal of Wind Engineering and Industrial Aerodynamics 2020; 207: 104398.
[15] Claus H, Schiehlen W, Modeling and simulation of railway bogie structural vibrations, Vehicle System Dynamics 1998; 29 (1): 538-552.